Molecular Mechanism of Spectral Tuning by Chloride Binding in Monkey Green Sensitive Visual Pigment

Kazuhiro J. Fujimoto[1,2], Fumika Minowa[2], Michiya Nishina[2], Shunta Nakamura[3], Sayaka Ohashi[3], Kota Katayama[3,4], Hideki Kandori[3,4*], and Takeshi Yanai[1,2]*

[1] Institute of Transformative Bio-Molecules (WPI-ITbM), Nagoya University, Furocho, Chikusa, Nagoya 464-8601, Japan

[2] Department of Chemistry, Graduate School of Science, Nagoya University, Furocho, Chikusa, Nagoya, 464-8601, Japan

[3] Department of Life Science and Applied Chemistry, Graduate School of Engineering, Nagoya Institute of Technology, Gokiso-cho, Showa, Nagoya, 466-8555, Japan

[4] OptoBioTechnology Research Center, Nagoya Institute of Technology, Gokiso-cho, Showa, Nagoya, 466-8555, Japan

Corresponding Authors

Kazuhiro J. Fuijmoto: fujimotok@chem.nagoya-u.ac.jp

Hideki Kandori: kandori@nitech.ac.jp

ABSTRACT

The visual pigments of the cones perceive red, green, and blue colors. The monkey green (MG) pigment possesses a unique Cl^- binding site; however, its relationship to the spectral tuning in green pigments remains elusive. Recently, FTIR spectroscopy revealed the characteristic structural modifications of the retinal binding site by Cl^- binding. Herein, we report the computational structural modeling of MG pigments and quantum-chemical simulation to investigate its spectral redshift and physicochemical relevance when Cl^- is present. Our protein structures reflect the previously suggested structural changes. AlphaFold2 failed to predict these structural changes. Excited-state calculations successfully reproduced the experimental red-shifted absorption energies, corroborating our protein structures. Electrostatic energy decomposition revealed that the redshift results from the His197 protonation state and conformations of Glu129, Ser202, and Ala308; however, Cl^- itself contributes to the blueshift. Site-directed mutagenesis supported our analysis. These modeled structures may provide a valuable foundation for studying cone pigments. (149/150 words)

TOC GRAPHICS

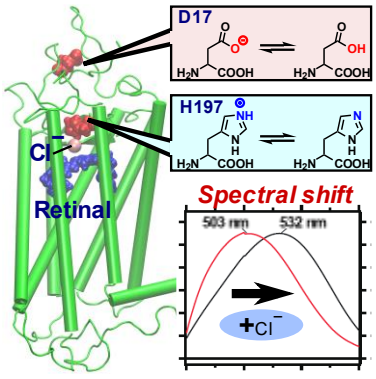

KEYWORDS: Protein structure prediction, Excited states, Quantum chemistry, Color vision, Mutagenesis experiments, Retinal proteins

Retinal proteins, which represent seven-transmembrane photoreceptors found in a variety of organisms from microbes to animals, including humans, serve crucial roles in the expression of biological functions, such as ion transport and vision[1-7]. The two major groups of retinal proteins responsible for vision are rhodopsin and cone pigments[4]. Rhodopsin distinguishes between darkness and light[8], whereas cone pigments perceive red, green, and blue colors with individually distinct absorption maxima[9]. The retinal chromophore is responsible for light absorption in these retinal proteins, suggesting that the protein environment surrounding the retinal chromophore contributes significantly to the differences in the absorption maxima.

Mammalian cone pigments are further divided into four groups, S, M1, M2, and L, based on the region of absorption maxima[4]. The L group, which contains the green and red cone pigments responsible for color vision, exhibited absorption maxima at longer wavelengths. FTIR experiments have confirmed that L-group proteins bind a chloride ion (Cl^-) near the retinal binding site[10], which is characteristic of the L group not observed in other cone pigments[11-13].

Several studies have determined the crystal structures of rhodopsin[14-19], but no experimental structures of cone pigments have been reported. This may be attributed to the low protein expression, which makes protein samples difficult to obtain. The extremely low thermal stability of cone pigments than that of rhodopsin is an additional impediment to conducting research. To obtain structural information on the cone pigments, two authors (K.K. and H.K.) and their collaborators successfully prepared a protein sample of monkey green (MG) cone pigment utilizing a mammalian (HEK293 cell line) expression system and performed FTIR experiments[20-23]. Spectral analysis revealed that Cl^- binding significantly altered the structure of MG near the retinal binding site. Additionally, they demonstrated that MG undergoes a 30 nm spectral redshift when transitioning from the Cl^- free form (λ_{max} = 503 nm) to the Cl^- bound form (λ_{max} = 532 nm).

These experimental results strongly suggest that Cl^- binding significantly contributes to the longer absorption wavelengths of L-group cone pigments. However, the molecular mechanism underlying the spectral shift associated with Cl^- binding remains unknown. As previously mentioned, one of the reasons for this is the absence of the three-dimensional structure of cone pigments.

Numerous theoretical studies based on quantum chemical calculations have been previously conducted on the mechanism of spectral tuning[24-27], wherein the retinal chromophore modulates absorption energy. However, fewer theoretical studies were performed on cone pigments[28-34] than on rhodopsin[35-46]. This is attributed to the unavailability of the crystal structures of the cone pigments. To circumvent this problem, one of the authors (K.J.F.) and his collaborators employed a computational method, called homology modeling[47], to predict the three-dimensional structure and analyzed the spectral tuning mechanism underlying human color vision[30, 31]. They observed that differences in the protein electrostatic potentials developed on the retinal π-chain were the primary source of changes in the absorption energies of red, green, and blue cone pigments. Furthermore, they demonstrated that the difference in the absorption energies between red and green cone pigments is mostly determined by the orientation of the OH groups of the three polar amino acids[31]. This result was consistent with the results of mutagenesis experiments conducted by Asenjo et al.[48], thus benefiting our understanding of the spectral tuning mechanism in L-group cone pigments. However, their study did not focus on the effects of Cl^- binding to L-group proteins on the absorption energy. Since then, several computational studies focusing on cone pigments[32-34] have been reported; however, none have discussed the effects of Cl^- binding on spectral shifts.

In this study, we aimed to elucidate the molecular mechanism underlying the spectral redshift induced by Cl^- binding in MG, an L-group cone pigment. Our computational approach consisted of two steps: construction of the MG protein structure and determination of its absorption energy in terms of protein electrostatic effects. Additionally, we experimentally measured spectral shifts using MG mutants to validate the computationally predicted amino acid contribution.

The initial structure of MG was constructed via homology modeling using the crystal structure of bovine rhodopsin (Protein Data Bank (PDB) ID: 1L9H[16]) as a template. For homology modeling, the MG and bovine rhodopsin sequences were aligned. The results are presented in **Figure S1** of the Supporting Information (SI). The characteristic amino acids of MG and bovine rhodopsin are summarized in **Figure 1a**, together with the corresponding amino acids for cone pigments other than MG. As shown, Asp17, Gln114, His197, and Lys200 in MG are conserved in L-type cone pigments but not in bovine rhodopsin, where they correspond to Gly3, Ser98, Glu181, and Gln184, respectively. The comparison thus enables us to deduce that these four amino acids unique to L-type cone pigments create a protein environment favoring Cl^- binding.

A homology model of MG was derived from sequence alignment; however, due to methodological limitations, this structure does not include a retinal chromophore or chloride ion. Therefore, a retinal chromophore was manually inserted at Lys312 in the resulting structure. Based on FITR experimental results, the chloride ion was placed in the vicinity of His197 in the Cl^- bound form[22].

To refine these structures, molecular dynamics (MD) simulations were performed, followed by geometry optimization using our own *N*-layered integrated molecular orbital and molecular mechanics (ONIOM) method[49]. **Figure 1b** depicts the three-dimensional structures of MG in the Cl^- bound and free forms constructed in this study. In addition to the presence or absence

of a chloride ion within the protein, these two structures differ in the protonation state of the amino acids. **Figure 1c** summarizes the protonation states of the charged amino acids in the Cl^- bound and free forms of MG: In the Cl^- bound form, His197 and Asp17 are cationic and anionic, respectively, whereas both are neutral in the Cl^- free form. As previously mentioned, these two amino acids are characteristic of the L-type cone pigments. Notably, in the Cl^- free form, the numbers of cations and anions do not match, but adding chloride ions to the protein surface neutralizes the charge balance of the entire system.

A comparison of the structures of the two MG proteins revealed a significant change in the loop structure around the retinal binding site, represented in orange in **Figure 1b**. The distance between the oxygen in the main chain of His197 and the nitrogen in the main chain of Ser202 was measured to represent the loop structure. **Figure 1b** demonstrates the distance to be 3.88 Å for the Cl^- bound form, whereas it was 7.14 Å for the Cl^- free form. This indicates that a β-sheet is produced in this loop region in the Cl^- bound form, whereas it is unfolded in the Cl^- free form. This result is consistent with our previous understanding based on the FTIR results[22]. As depicted in **Figure 1a**, bovine rhodopsin also exhibits a loop structure formed by β-sheets near the retinal binding site. The distance between the β-strands forming this loop structure was measured to be 4.14 Å. **Figure S2** depicts the structural superposition of MG and bovine rhodopsin, confirming that structure of bovine rhodopsin is more similar to the Cl^- bound form than the Cl^- free form.

(a)

Residue Number in Bovine Rhodopsin	3	98	113	181	184	190	268	296
Residue Number in Monkey Green	17	114	129	197	200	206	284	312
Bovine Rhodopsin	G	S	E	E	Q	D	Y	K
Chicken Green	G	A	E	E	Q	D	Y	K
Chicken Blue	T	F	E	E	Q	D	Y	K
Chicken Violet	M	S	E	E	Q	D	Y	K
Human Blue	M	S	E	E	Q	D	Y	K
Monkey Blue	M	S	E	E	Q	D	Y	K
Marmoset Blue	M	S	E	E	Q	D	Y	K
Monkey Green	D	Q	E	H	K	D	Y	K
Monkey Red	D	Q	E	H	K	D	Y	K
Human Green	D	Q	E	H	K	D	Y	K
Human Red	D	Q	E	H	K	D	Y	K
Zebrafish Red	D	Q	E	H	K	D	Y	K
Chicken Red	E	Q	E	H	K	D	Y	K
Xenopus Red	D	Q	E	H	K	D	Y	K
Snake Red	D	Q	E	H	K	D	Y	K
Lizard Red	D	Q	E	H	K	D	Y	K

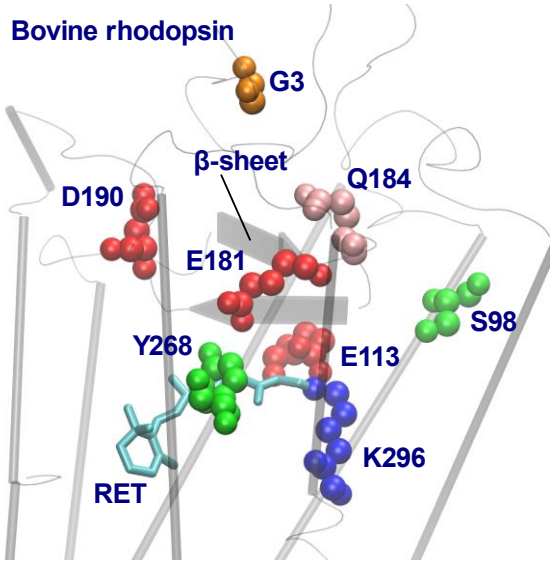

(b)

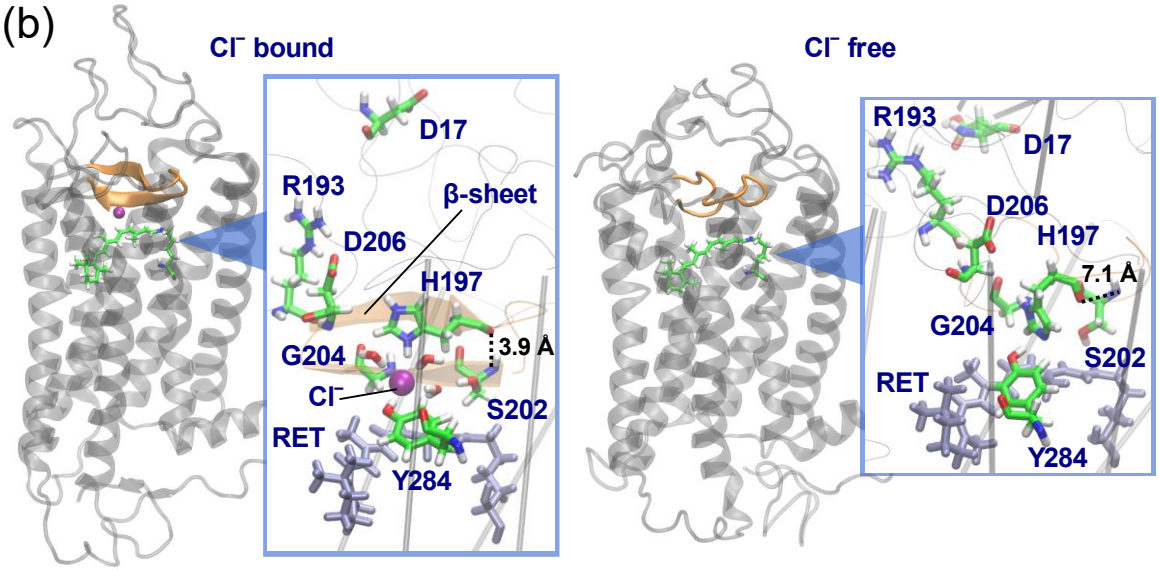

(c)

	Protonation state	
	Cation	Anion
Cl^- bound	H197, K200, K312, R13, R37, R193	D17, D21, D206, E20, E129, Cl^-
Cl^- free	K200, K312, R13, R37, R193	D21, D206, E20, E129

(d)

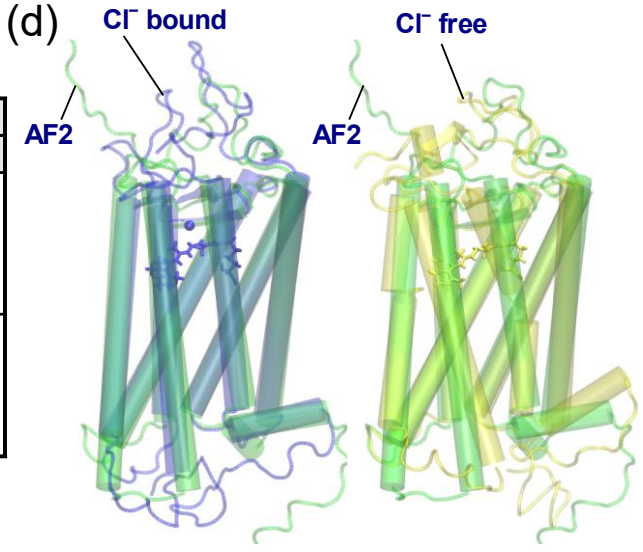

Figure 1. (a) Comparison of amino acids among bovine rhodopsin, MG, and other cone pigments. The crystal structure of bovine rhodopsin illustrates each amino acid (PDBID: 1L9H[16]). (b) Computationally constructed MG structures in the Cl^- bound (left) and free (right) forms. Orange represents the β-sheet structure in the loop region near the retinal chromophore. The detailed structure around the Cl^- binding site is also shown. His197, Gly204, Tyr284, and three water molecules interact with the chloride ion. (c) The protonation state of each amino acid in the Cl^- bound and free forms of MG employed in the calculations. (d) Comparison of the MG structure predicted by AlphaFold2 with our constructed structures. Left: superposition of the AlphaFold2 structure and our Cl^- bound structure, right: superposition of the AlphaFold2 structure and our Cl^- free structure.

In the Cl^- bound form, His197, an amino acid in close proximity to the chloride ion, is protonated to a cationic state. Conversely, in the Cl^- free form, His197 is deprotonated to a charge-neutral state. In contrast, the Cl^- free form of Asp17 may be anionic (COO^-) or neutral (COOH). Therefore, we attempted to develop a comparable computational model for the scenario wherein Asp17 is anionic in the Cl^- free form. The resulting structure resembled the Cl^- bound form, with the loop structure near the retinal binding site folded in the β-sheet; however, this loop structure was significantly unfolded when Asp17 was neutralized (see **Figure S3** for details). Thus, these calculations strongly suggest that the difference in the protonation state of Asp17 is crucial for the structural change between the Cl^- bound and free forms of the loop.

The structure of the Cl^- binding site was then investigated. As illustrated in **Figure 1b** and **Figure S4**, the chloride ion is stabilized by the interaction of His197, Tyr284, Gly204, and three additional water molecules in an octahedral configuration. His197 has been previously reported as

the counter ion of the chloride ion[50], but the interaction of Tyr284 and Gly204 with the chloride ion has not been studied. In addition to His197, the present calculations strongly suggest that Tyr284 and Gly204, play key roles in the Cl^- binding of MG.

In recent years, AlphaFold2 has garnered significant attention as a computational method for highly accurate prediction of three-dimensional protein structures[51]. We compared the structure determined by our method with that predicted by AlphaFold2. Notably, neither retinal nor chloride ions are present in the structure predicted by AlphaFold2, as AlphaFold2 could only handle amino acids. Therefore, the AlphaFold2 structure corresponds to that of the Cl^- free form. However, as illustrated in **Figure 1d**, the structure of MG as determined by AlphaFold2 differed from our structure of the Cl^- free form. The loop region near the retinal binding site was not unfolded in the AlphaFold2 structure. These results indicate that AlphaFold2 has not yet achieved reliable modeling of chromophores- or ion-containing proteins.

Absorption energy calculations using the symmetry-adapted cluster-configuration interaction (SAC-CI) method[52] were performed on the constructed MG structures in the Cl^- bound and free forms. Both the Cl^- bound and free forms of MG exhibited large oscillator strengths f in the first excited states (f = 1.05 and 1.08 for the Cl^- bound and free forms, respectively), indicating π–π^* excitations with the highest occupied molecular orbital (HOMO) to lowest unoccupied molecular orbital (LUMO) transition as the main configuration, consistent with our previous results for retinal proteins[42]. As reported in **Figure 2a**, SAC-CI calculations yielded excitation energies of 2.43 and 2.32 eV for the Cl^- free and bound forms, respectively, matching the experimental values (Cl^- free: 2.47 eV (503 nm), Cl^- bound: 2.33 eV (532 nm)) with a deviation of 0.01-0.04 eV. Notably, the present excited-state calculations exhibited a spectral redshift of 0.11 eV from the Cl^- free form to the Cl^- bound form, thereby reproducing the experimental value of

0.14 eV (**Figure 2b**). Additionally, we calculated the absorption energies using time-dependent density functional theory with the CAM-B3LYP functional (TD-CAM-B3LYP)[53] and the complete active space second-order perturbation theory (CASPT2)[54] (**Figure 2a**) and discovered that the spectral redshift resulting from Cl^- binding was also observed in these calculations (**Figure 2b**), although the magnitude of the spectral shift was marginally different (TD-CAM-B3LYP: 0.08 eV and CASPT2: 0.12 eV). Thus, the redshift induced by Cl^- binding results from our protein structures and is independent of the electronic structure calculations. These calculations strongly supported the validity of the MG structures.

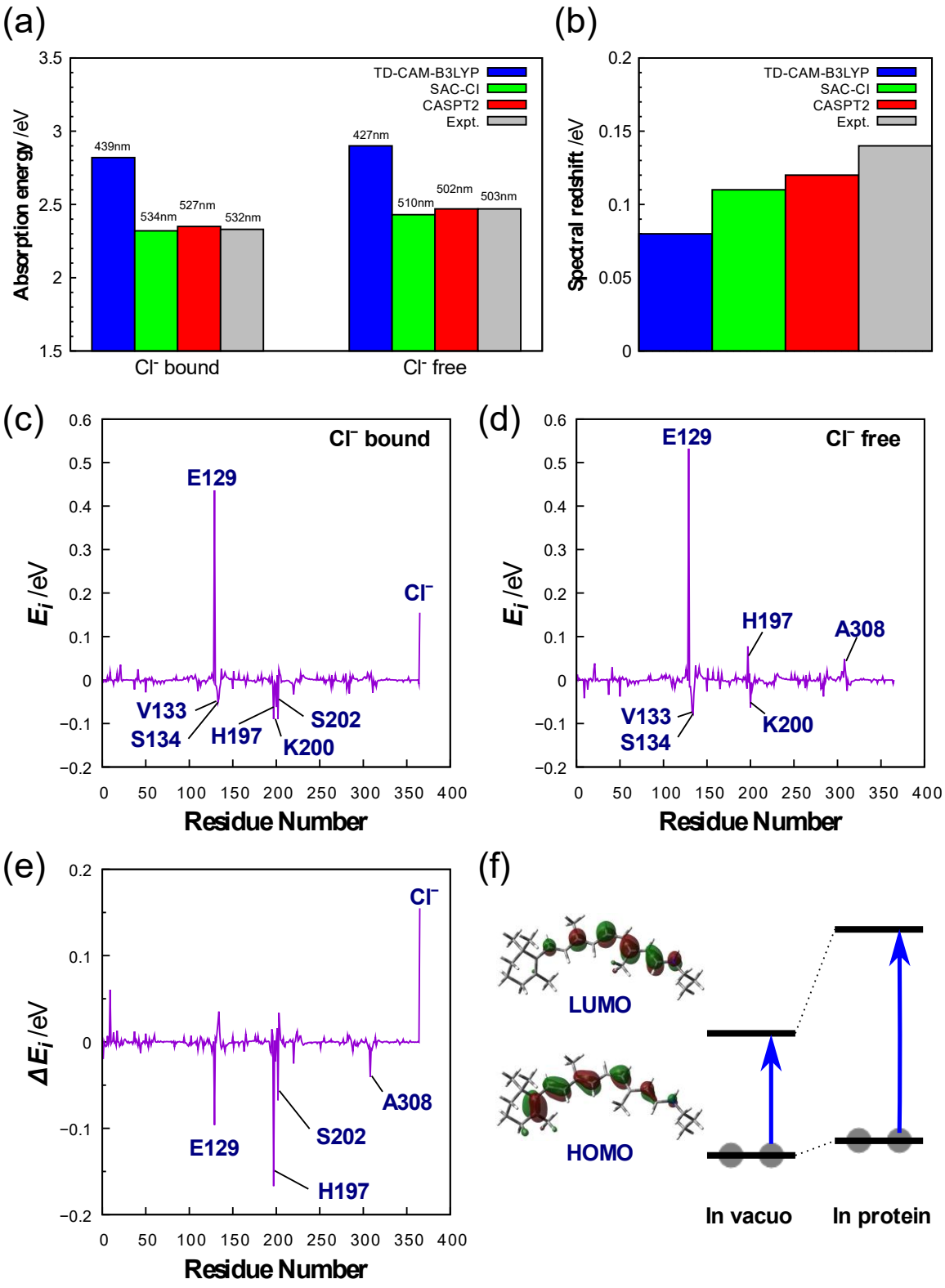
(a)
Absorption energy /eV
TD-CAM-B3LYP
SAC-CI
CASPT2
Expt.
439nm
534nm
527nm
532nm
427nm
510nm
502nm
503nm
Cl⁻ bound
Cl⁻ free
(b)
Spectral redshift /eV
(c)
Cl⁻ bound
E129
Cl⁻
V133
S134
H197
S202
K200
Residue Number
(d)
Cl⁻ free
E129
H197
A308
V133
S134
K200
Residue Number
(e)
ΔEi /eV
Cl⁻
A308
E129
S202
H197
Residue Number
(f)
LUMO
HOMO
In vacuo
In protein

Figure 2. (a) Absorption energies calculated for the Cl^- bound and free forms of MG using the TD-CAM-B3LYP, SAC-CI, and CASPT2 methods. (b) The calculated spectral redshift associated with Cl^- binding of MG. The absorption energy values in (a) are used. The contribution of the electrostatic effect of each amino acid to the absorption energy of MG in (c) Cl^- bound and (d) Cl^- free forms. (e) The contribution of each amino acid to the spectral shift induced by Cl^- binding. Positive and negative values represent the contribution to the spectral blueshift and redshift, respectively. (f) Schematic illustration of the orbital energy changes of retinal due to protein electrostatic effects. Based on the difference in the distribution of HOMO and LUMO, the first excited state of the retinal exhibits an intramolecular CT character. Therefore, the LUMO is specifically destabilized by the negative electrostatic potential from the protein in the vicinity of the retinal Schiff base, thereby increasing the HOMO–LUMO gap.

We investigated the physicochemical contributions that generate spectral differences in the Cl^- bound and free forms based on the accurate reproduction of the absorption energies. To achieve this, the electrostatic energy contribution of each amino acid in the MG protein was calculated. The contribution of each amino acid to the absorption energy is determined from the electrostatic energy difference between the excited and ground states of the retinal chromophore, as follows:

$$E_i = \sum_{a \in i} \sum_{b \in \mathrm{Retinal}} \frac{Q_a \left(q_b^{\mathrm{e}} - q_b^{\mathrm{g}} \right)}{r_{ab}} , \quad (1)$$

where Q_a denotes the atomic charge of atom *a* in amino acid *i*, q_b^{e} and q_b^{g} represent the charges of atom *b* in the retinal chromophore in the excited and ground states, respectively, and r_{ab} is the interatomic distance between the retinal and amino acid *i*. In this study, E_i represents the protein

electrostatic energy. **Figures 2c** and **2d** illustrate the contribution of each amino acid to the MG absorption energy in Cl^- bound and free forms, respectively. The positive and negative values on the *y*-axis indicate blueshift and redshift contributions to the optical absorption of the retinal chromophore as a function of amino acids, respectively. The combined contribution from each amino acid is positive for both the Cl^- bound and free forms, indicating that the electrostatic effect of the entire protein contributes to the blueshift. This finding is consistent with our previous results[30]. Because the first excited state of the retinal chromophore possesses an intramolecular charge transfer (CT) character along the retinal π-chain, the LUMO of the retinal chromophore is specifically destabilized when the protein electrostatic potential is applied along the retinal π-chain[42] (**Figure 2f**). Thus, the HOMO–LUMO gap increased, contributing to the spectral blueshift. **Figure 2c** depicts that the Cl^- bound form exhibits substantial blueshifts owing to Glu129 and the chloride ion, and large redshifts owing to Val133, Ser134, His197, Lys200, and Ser202. In contrast, a large blueshift owing to Glu129 and His197 and a large redshift owing to Val133, Ser134, and Lys200 were observed in the Cl^- free form, as illustrated in **Figure 2d**. Notably, the Cl^- free form does not include the contribution from the chloride ion, and the change in the His197 protonation state results in the opposite contribution to the spectral shift than the Cl^- bound form. All the amino acids discussed herein were close to the retinal binding site.

To further investigate the effect of Cl^- binding, the difference in the protein electrostatic energy E_i between the Cl^- bound and free forms was calculated as follows:

$$\Delta E_i = E_i^{\text{Bound}} - E_i^{\text{Free}} \quad , \quad (2)$$

where E_i^{Bound} and E_i^{Free} represent the protein electrostatic energy of an amino acid i in the Cl^- bound and free forms, respectively. Calculating ΔE_i assists in determining which amino acids

contribute to the spectral redshift from the Cl^- free form to the Cl^- bound form. Notably, Eq. (2) uses the value of the Cl^- free form as the reference value; therefore, the positive and negative values of ΔE_i imply a contribution to the blueshift and redshift after Cl^- binding, respectively. As depicted in **Figure 2e**, the largest negative value of ΔE_i was observed at His197 (−0.167 eV), indicating that His197 was the largest redshift contributor induced by Cl^- binding. As previously mentioned, His197 is considered a cation in the Cl^- bound form and neutral in the Cl^- free form. This difference in the protonation state brings a substantial contribution to the spectral shift. In addition to His197, large redshift contributions were observed for Glu129 (−0.096 eV), Ser202 (−0.067 eV), and A308 (−0.041 eV). In contrast, the chloride ion exhibited the largest positive value of ΔE_i (0.154 eV), which contradicts our intuition that the chloride ion itself contributes to the redshift. As stated previously, the counterion of Cl^- is His197; therefore, considering His197 and Cl^- as a single fragment, their combined contributions yield a negative value of −0.013 eV. These results indicate that although the sole direct contribution of Cl^- is the blueshift, the pair of Cl^- and His197 contribute to the redshift by altering the protonation state of His197 to a cation through Cl^- binding.

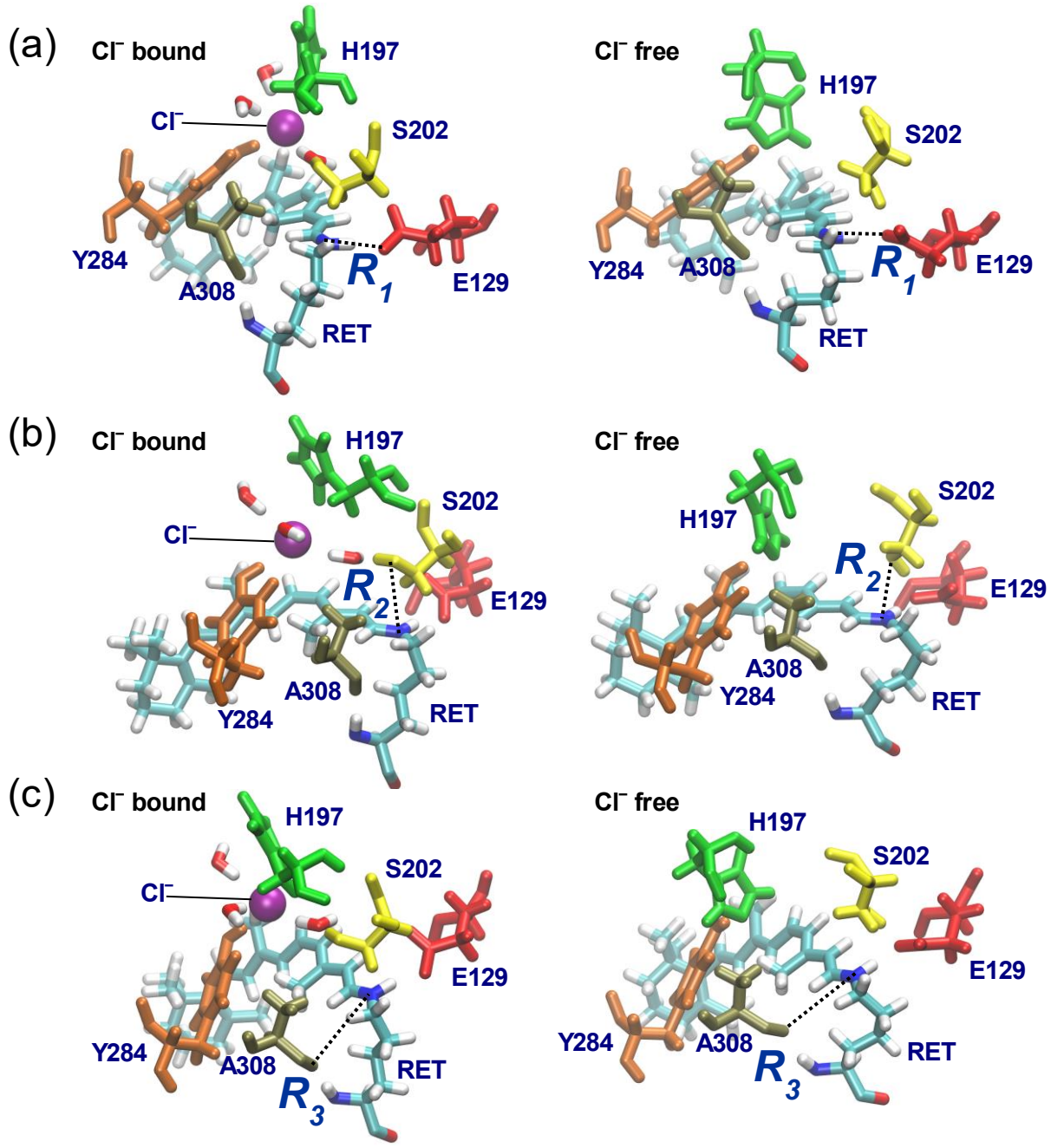

Figure 3. Structural comparison of Cl^- bound and Cl^- free forms of (a) Glu129, (b) Ser202, and (c) Ala308. R_1, R_2, and R_3 are the distances between the oxygen of the carboxyl group in Glu129 and the nitrogen of the retinal Schiff base, the oxygen of the OH group in Ser202 and the nitrogen of the retinal Schiff base, and the oxygen of the carbonyl group in Ala308

and the nitrogen of the retinal Schiff base, respectively. R_1 = 2.76 Å, R_2 = 4.12 Å, and R_3 = 4.56 Å in the Cl^- bound form, and R_1 = 2.74 Å, R_2 = 3.25 Å, and R_3 = 4.37 Å in the Cl^- free form.

The analysis using Eq. (2) demonstrates that His197 is a single amide with the largest contribution to the redshift. However, the second, third, and fourth largest, which originate from Glu197, Ser202, and A308, respectively, are especially the most effective because they are larger than the combined contributions of His197 and Cl^-. The combined spectral shift from these three amino acids was −0.204 eV, indicating that they accounted for a large contribution to the overall spectral shift of the protein (−0.161 eV). Therefore, we analyzed the molecular mechanism underlying the large redshift contributions of Glu197, Ser202, and A308. First, we compared the Glu129 structure between the Cl^- bound and free forms. As depicted in **Figure 3a**, a difference was observed in the carboxyl group orientations of Glu129 between the Cl^- bound and free forms. The distance between the oxygen of the carboxyl group and the nitrogen of the retinal Schiff base is defined as R_1, and R_1 = 2.74 and 2.76 Å for the Cl^- free and bound forms, respectively. In the Cl^- bound form, the negatively charged carboxyl group is distant from the retinal Schiff base, indicating that the negative electrostatic potential developed on the retinal π-chain is smaller. Thus, the redshift contribution of Glu129 results from the weakening of the negative electrostatic potential in the Cl^- bound form relative to the Cl^- free form. Next, the Ser202 structure was compared between Cl^- bound and free forms. As illustrated in **Figure 3b**, a significant difference was observed in the OH group position. The OH group of Ser202 in the Cl^- free form is close to the retinal π-chain, and R_2, defined as the distance between the oxygen of the OH group and nitrogen of the retinal Schiff base, is 3.25 Å. In contrast, the OH group of Ser202 in the Cl^- bound

form was distant from the retinal Schiff base (R_2 = 4.12 Å) because of hydrogen bond formations with the water molecule coordinated to the chloride ion. The oxygen atom of the OH group in serine is polarized to a negative charge. Thus, the position change of the OH group of Ser202 relative to the retinal Schiff base leads to a difference in the magnitude of the electrostatic potential, resulting in a spectral shift. A similar analysis of Ala308 (**Figure 3c**) exhibited a difference in R_3, defined as the distance between the carbonyl oxygen (C=O) of the main chain of Ala308 and the nitrogen of the retinal Schiff base: in the Cl^- free form, R_3 = 4.37 Å, whereas in the Cl^- bound form R_3 = 4.56 Å. Because the carbonyl oxygen is also polarized to a negative charge, the shifting away of the carbonyl oxygen of A308 from the retinal Schiff base in the Cl^- bound form weakens the effect of the negative electrostatic potential, thereby leading to a redshift. These calculations suggest that the redshift owing to Cl^- binding results from the weakening of the negative electrostatic potential developed on the retinal π-chain, especially near the Schiff base region, owing to conformational changes in the amino acids around the retinal binding site.

Computational prediction of the MG structure and spectral shift analysis allowed us to identify the amino acids involved in the spectral shift associated with Cl^- binding. To verify the effects of these amino acids, site-directed mutagenesis experiments on MG were performed and their absorption spectra were compared with those of the wild type (WT). The absorption spectra measured for the 17 MG mutants are depicted in **Figure 4**. Considering the Cl^- bound form, the absorption maxima of A308S (λ_{max} = 501 nm) and H197A (λ_{max} = 504 nm) exhibited a substantial blueshift compared with that of the WT (λ_{max} = 532 nm). This indicated that Ala308 and His197 were significantly involved in Cl^- binding. To further investigate the amino acids involved in the redshift induced by Cl^- binding, the magnitude of the spectral shift from the NO^{3-} bound form, which mimics the Cl^- free form[22, 23], to the Cl^- bound form was estimated for each mutant, defined

by $\Delta = \lambda_{max}^{Bound} - \lambda_{max}^{Free}$. If the spectral shift of the mutant is smaller than that of the WT, the mutated amino acid is considered to be directly involved in the Cl^- binding-induced redshift. The analysis revealed that the spectral shifts Δ in H197A, H197Y, S202A, and A308S (−0.03, −0.05, −0.04, and −0.06 eV) were significantly smaller than those in the WT (−0.14 eV), strongly suggesting that His197, Ser202, and Ala308 are largely responsible for the redshift associated with Cl^- binding in the MG. This result is consistent with the predictions of the computational analysis described earlier. Therefore, the mutagenesis experiments confirmed the high reliability of our computational prediction of amino acid contributions.

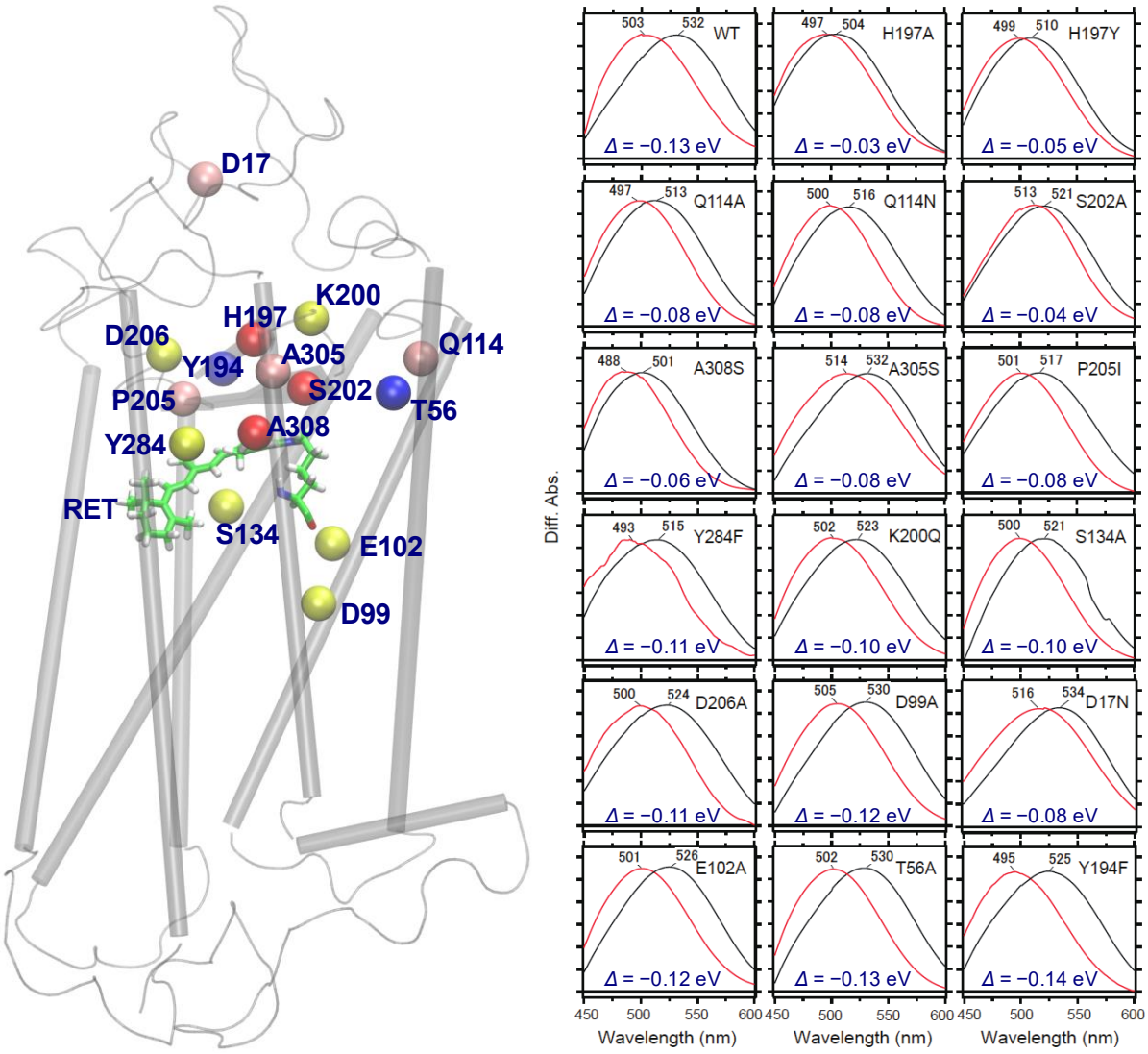

Figure 4. Absorption spectra of MG mutants. Black and red lines represent absorption spectra in Cl^- bound and NO^{3-} bound forms, respectively, and the difference in absorption maxima ($\Delta = \lambda_{max}^{Bound} - \lambda_{max}^{Free}$) is also depicted. The position of each amino acid within the MG structure is indicated by a sphere. Spheres indicating amino acids are represented by red, pink, yellow, and blue in the order of magnitude of the redshift.

In summary, the molecular mechanism of the spectral redshift associated with Cl^- binding was clearly demonstrated by computationally constructing the protein structures of Cl^- bound and free MGs and by analyzing the electrostatic energy of the proteins. This study demonstrated for the first time that a change in the loop structure of MG cannot be reproduced by the presence or absence of a chloride ion alone, but is rather caused by a change in the protonation state of both His197 and Asp17 (**Figure 5**). The binding of a chloride ion to MG alters the protonation state and conformation of the amino acids (His197, Glu129, Ser202, Ala308) surrounding the retinal binding site, thereby weakening the negative electrostatic potential developed near the retinal Schiff base and producing a spectral redshift. The computationally predicted amino acid contributions were in excellent agreement with the results of the mutagenesis experiments, indicating that this study has made a significant contribution toward elucidating the spectral tuning mechanism of cone pigments.

As shown in **Figure 4**, the experimental spectra of the MG mutants showed a spectral shift relative to that of the WT even in the absence of Cl^- binding. This suggests that factors other than Cl^- binding, such as retinal distortion and the hydroxyl dipole, contribute to spectral tuning. Although it would be interesting to investigate the cause of the spectral shift in detail, this would require further structural construction of the MG mutants. Such studies will be conducted in our future work.

Finally, we compare the spectral tuning of MG with that of other photobiomolecules. We previously investigated the molecular mechanism of the spectral shift between the inner (B850) and outer rings (B800) constituting the photosynthetic light-harvesting 2 complex (LH2) of purple bacteria and found that electronic coupling and CT between chromophores are the major

contributors to the spectral shift, whereas the electrostatic effect from the protein environment is a only minor one[55] (e.g., **Figure 6** of Ref. 55). In contrast, this study demonstrates that protein electrostatic effect induces the spectral tuning of MG. These results imply that the physicochemical factors underlying the spectral tuning of MG and LH2 are essentially different. As shown in **Figure 2f** and in our previous studies[42, 56] (e.g., **Figure 3** of Ref. 42 and **Figure 2** of Ref. 56), the first excited state of the retinal chromophore has an intramolecular CT character. Consequently, the retinal chromophore is highly sensitive to the electrostatic potential from the protein environment and thus exhibits a spectral shift. In contrast, the excited states of chromophores such as bacteriochlorophylls and carotenoids in LH2 exhibit minimal intramolecular CT; thus, the spectra of these chromophores are less affected by the electrostatic potential from the protein environment. These findings support the hypothesis that biomolecules employ different physicochemical strategies to modulate their absorption wavelengths and enhance their adaptation to the living environment.

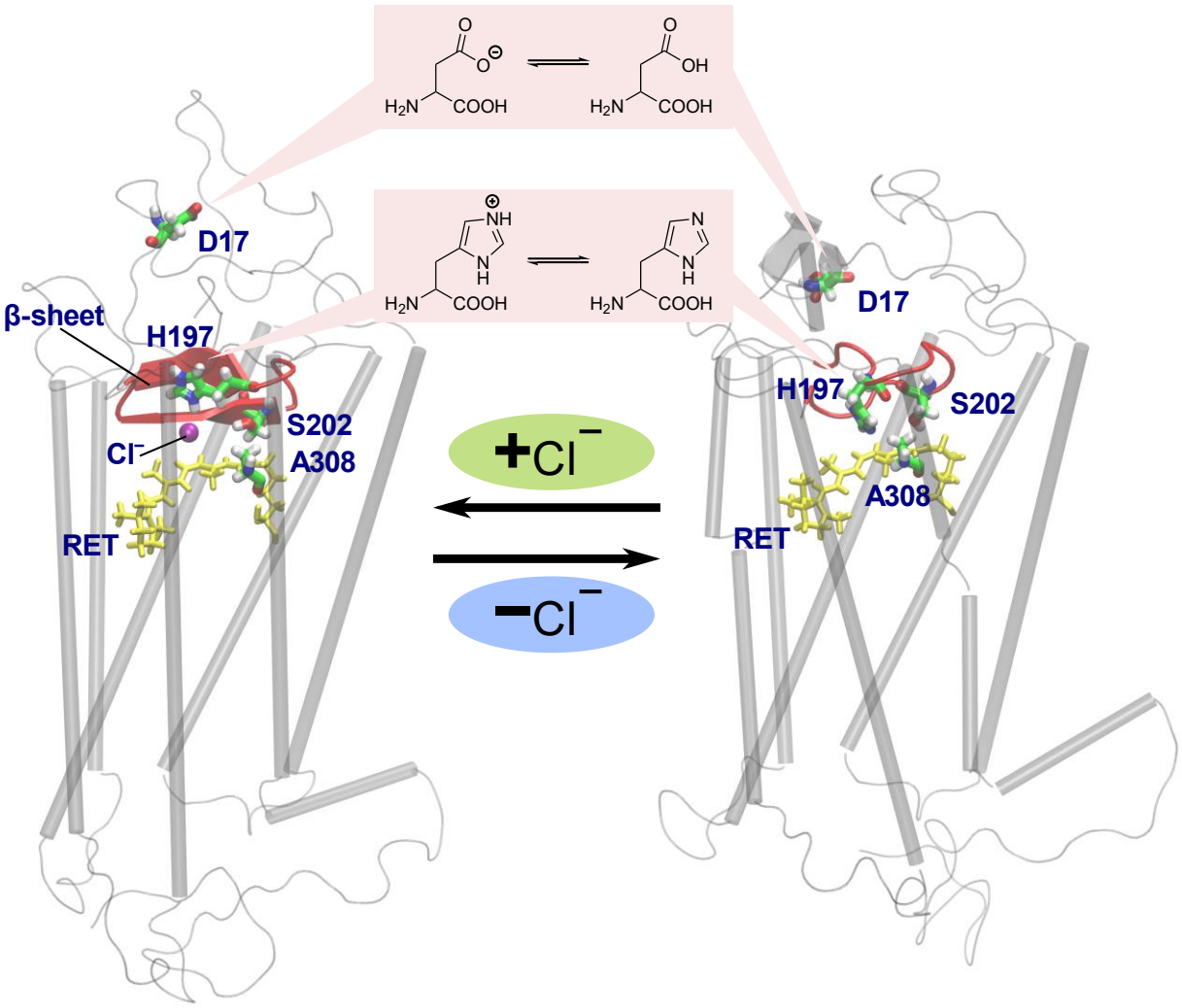

Figure 5. Schematic illustration of the changes in the protonation state and protein structure induced by Cl^- binding.

ASSOCIATED CONTENT

Supporting Information

The following files are available free of charge.

Details of the computational procedures for the construction of the three-dimensional structures

of the MG proteins and the calculation of their excited states; details of the experimental procedures for the expression of WT and mutant MG proteins, the measurement of their absorption spectra; additional figures of sequence alignment between MG and bovine rhodopsin (Figure S1); superimposed structures of MG and rhodopsin (Figure S2); Cl^- free MG structure for anionic Asp17 (Figure S3); structure of Cl^- binding site (Figure S4); and plots of active orbitals used for the CASPT2 calculations (Figure S5) (PDF).

Atomic coordinates of Cl^- bound and free MG structures (PDB).

AUTHOR INFORMATION

Corresponding Authors

Kazuhiro J. Fujimoto – orcid.org/0000-0003-0286-3646; E-mail: fujimotok@chem.nagoya-u.ac.jp

Hideki Kandori – orcid.org/0000-0002-4922-1344; E-mail: kandori@nitech.ac.jp

Notes

The authors declare no competing financial interests.

ACKNOWLEDGMENT

This study was supported by JSPS KAKENHI (Grant Nos. 20K05430 to KJF, 21H01881 and JP21K18931 to TY, 18K14662 and 20H05440 to KK, and 21H04969 to HK), JST, CREST (Grant No. JPMJCR21O5 to KJF), and PRESTO (Grant No. JPMJPR19G4 to KK).

REFERENCES

(1) Wald, G., Molecular Basis of Visual Excitation. *Science* **1968**, 162, 230-239.

(2) Birge, R. R., Nature of the primary photochemical events in rhodopsin and bacteriorhodopsin. *Biochim. Biophys. Acta* **1990**, 1016, 293-327.

(3) Callender, R.; Honig, B., RESONANCE RAMAN STUDIES OF VISUAL PIGMENTS. *Ann. Rev. Biophys. Bioeng.* **1977**, 6, 33-55.

(4) Shichida, Y.; Imai, H., Visual pigment: G-protein-coupled receptor for light signals. *Cell. Mol. Life Sci.* **1998**, 54, 1299-1315.

(5) Hampp, N., Bacteriorhodopsin as a Photochromic Retinal Protein for Optical Memories. *Chem. Rev.* **2000**, 100, 1755-1776.

(6) Mathies, R. A.; Lugtenburg, J. Chapter 2 the Primary Photoreaction of Rhodopsin. In *Handbook of Biological Physics*, Stavenga, D. G.; Grip, W. J. d.; Pugh, E. N., Eds.; Elsevier Science B. V.: Amsterdam, 2000; Vol. 3, pp 55-90.

(7) Ernst, O. P.; Lodowski, D. T.; Elstner, M.; Hegemann, P.; Brown, L. S.; Kandori, H., Microbial and Animal Rhodopsins: Structures, Functions, and Molecular Mechanisms. *Chem. Rev.* **2014**, 114, 126-163.

(8) Kandori, H.; Schichida, Y.; Yoshisawa, T., *Biochemistry (Moscow)* **2001**, 66, 1197.

(9) Kochendoerfer, G. G.; Lin, S. W.; Sakmar, T. P.; Mathies, R. A., How color visual pigments are tuned. *Trends. Biochem. Sci.* **1999**, 24, 300-305.

(10) Hirano, T.; Imai, H.; Kandori, H.; Shichida, Y., Chloride Effect on Iodopsin Studied by Low-Temperature Visible and Infrared Spectroscopies. *Biochemistry* **2001**, 40, 1385-1392.

(11) Knowles, A., The effects of chloride ion upon chicken visual pigments. *Biochem. Biophys. Res. Commun.* **1976**, 73, 56-62.

(12) Fager, L. Y.; Fager, R. S., Halide control of color of the chicken cone pigment iodopsin. *Exp. Eye Res.* **1979**, 29, 401-408.

(13) Shichida, Y.; Kato, T.; Sasayama, S.; Fukada, Y.; Yoshizawa, T., Effects of chloride on chicken iodopsin and the chromophore transfer reactions from iodopsin to scotopsin and B-photopsin. *Biochemistry* **1990**, 29, 5843-5848.

(14) Palczewski, K.; Kumasaka, T.; Hori, T.; Behnke, C. A.; Motoshima, H.; Fox, B. A.; Trong, I. L.; Teller, D. C.; Okada, T.; Stenkamp, R. E., et al., Crystal Structure of Rhodopsin: A G Protein-Coupled Receptor. *Science* **2000**, 289, 739-745.

(15) Teller, D. C.; Okada, T.; Behnke, C. A.; Palczewski, K.; Stenkamp, R. E., Advances in Determination of a High-Resolution Three-Dimensional Structure of Rhodopsin, a Model of G-Protein-Coupled Receptors (GPCRs). *Biochemistry* **2001**, 40, 7761-7772.

(16) Okada, T.; Fujiyoshi, Y.; Silow, M.; Navarro, J.; Landau, E. M.; Shichida, Y., Functional role of internal water molecules in rhodopsin revealed by x-ray crystallography. *Proc. Natl. Acad. Sci. USA* **2002**, 99, 5982-5987.

(17) Okada, T.; Sugihara, M.; Bondar, A.; Elstner, M.; Entel, P.; Buss, V., The Retinal Conformation and its Environment in Rhodopsin in Light of a New 2.2 Å Crystal Structure. *J. Mol. Biol.* **2004**, 342, 571-583.

(18) Li, J.; Edwards, P. C.; Burghammer, M.; Villa, C.; Schertler, G. F. X., Structure of Bovine Rhodopsin in a Trigonal Crystal Form. *J. Mol. Biol.* **2004**, 343, 1409-1438.

(19) Makino, C. L.; Riley, C. K.; Looney, J.; Crouch, R. K.; Okada, T., Binding of More Than One Retinoid to Visual Opsins. *Biophys. J.* **2010**, 99, 2366-2373.

(20) Katayama, K.; Furutani, Y.; Imai, H.; Kandori, H., An FTIR Study of Monkey Green- and Red-Sensitive Visual Pigments. *Angew. Chem. Int. Ed.* **2010**, 49, 891-894.

(21) Katayama, K.; Furutani, Y.; Imai, H.; Kandori, H., Protein-Bound Water Molecules in Primate Red- and Green-Sensitive Visual Pigments. *Biochemistry* **2012**, 51, 1126-1133.

(22) Katayama, K.; Furutani, Y.; Iwaki, M.; Fukuda, T.; Imai, H.; Kandori, H., ‘‘In situ’’ observation of the role of chloride ion binding to monkey green sensitive visual pigment by ATR-FTIR spectroscopy. *Phys. Chem. Chem. Phys.* **2018**, 20, 3381-3387.

(23) Katayama, K.; Nakamura, S.; Sasaki, T.; Imai, H.; Kandori, H., Role of Gln114 in Spectral Tuning of a Long-Wavelength Sensitive Visual Pigment. *Biochemistry* **2019**, 58, 2944-2952.

(24) Warshel, A., Calculations of chemical processes in solutions. *J. Phys. Chem.* **1979**, 83, 1640-1652.

(25) Houjou, H.; Inoue, Y.; Sakurai, M., Physical Origin of the Opsin Shift of Bacteriorhodopsin. Comprehensive Analysis Based on Medium Effect Theory of Absorption Spectra. *J. Am. Chem. Soc.* **1998**, 120, 4459-4470.

(26) Hayashi, S.; Tajkhorshid, E.; Pebay-Peyroula, E.; Royant, A.; Landau, E. M.; Navarro, J.; Schulten, K., Structural Determinants of Spectral Tuning in Retinal ProteinsBacteriorhodopsin vs Sensory Rhodopsin II. *J. Phys. Chem. B* **2001**, 105, 10124-10131.

(27) Vreven, T.; Morokuma, K., Investigation of the S0 S1 excitation in bacteriorhodopsin with the ONIOM(MO:MM) hybrid method. *Theor. Chem. Acc.* **2003**, 109, 125-132.

(28) Trabanino, R. J.; Vaidehi, N.; Goddard, W. A., III, Exploring the Molecular Mechanism for Color Distinction in Humans. *J. Phys. Chem. B* **2006**, 110, 17230-17239.

(29) Fujimoto, K.; Hasegawa, J.; Hayashi, S.; Nakatsuji, H., On the color-tuning mechanism of Human-Blue visual pigment: SAC-CI and QM/MM study. *Chem. Phys. Letts.* **2006**, 432, 252-256.

(30) Fujimoto, K.; Hasegawa, J.; Nakatsuji, H., Origin of color tuning in human red, green, and blue cone pigments: SAC-CI and QM/MM study. *Chem. Phys. Letts.* **2008**, 462, 318-320.

(31) Fujimoto, K.; Hasegawa, J.; Nakatsuji, H., Color Tuning Mechanism of Human Red, Green, and Blue Cone Pigments: SAC-CI Theoretical Study. *Bull. Chem. Soc. Jpn.* **2009**, 82, 1140-1148.

(32) Altun, A.; Yokoyama, S.; Morokuma, K., Color Tuning in Short Wavelength-Sensitive Human and Mouse Visual Pigments: Ab initio Quantum Mechanics/Molecular Mechanics Studies. *J. Phys. Chem. A* **2009**, 113, 11685-11692.

(33) Frähmcke, J. S.; Wanko, M.; Elstner, M., Building a Model of the Blue Cone Pigment Based on the Wild Type Rhodopsin Structure with QM/MM Methods. *J. Phys. Chem. B* **2012**, 116, 3313-3321.

(34) Sekharan, S.; Katayama, K.; Kandori, H.; Morokuma, K., Color Vision: "OH-Site" Rule for Seeing Red and Green. *J. Am. Chem. Soc.* **2012**, 134, 10706-10712.

(35) Ferré, N.; Olivucci, M., Probing the Rhodopsin Cavity with Reduced Retinal Models at the CASPT2//CASSCF/AMBER Level of Theory. *J. Am. Chem. Soc.* **2003**, 125, 6868-6869.

(36) Andruniów, T.; Ferré, N.; Olivucci, M., Structure, initial excited-state relaxation, and energy storage of rhodopsin resolved at the multiconfigurational perturbation theory level. *Proc. Natl. Acad. Sci. USA* **2004**, 101, 17908-17913.

(37) Hufen, J.; Sugihara, M.; Buss, V., How the Counterion Affects Ground- and Excited-State Properties of the Rhodopsin Chromophore. *J. Phys. Chem. B* **2004**, 108, 20419-20426.

(38) Wanko, M.; Hoffmann, M.; Strodel, P.; Koslowski, A.; Thiel, W.; Neese, F.; Frauenheim, T.; Elstner, M., Calculating Absorption Shifts for Retinal Proteins: Computational Challenges. *J. Phys. Chem. B* **2005**, 109, 3606-3615.

(39) Coto, P. B.; Strambi, A.; Ferré, N.; Olivucci, M., The color of rhodopsins at the ab initio multiconfigurational perturbation theory resolution. *Proc. Natl. Acad. Sci. USA* **2006**, 103, 17154-17159.

(40) Gascón, J. A.; Sproviero, E. M.; Batista, V. S., Computational Studies of the Primary Phototransduction Event in Visual Rhodopsin. *Acc. Chem. Res.* **2006**, 39, 184-193.

(41) Sekharan, S.; Sugihara, M.; Buss, V., Origin of Spectral Tuning in Rhodopsin—It Is Not the Binding Pocket. *Angew. Chem. Int. Ed.* **2007**, 46, 269-271.

(42) Fujimoto, K.; Hayashi, S.; Hasegawa, J.; Nakatsuji, H., Theoretical Studies on the Color-Tuning Mechanism in Retinal Proteins. *J. Chem. Theory Comput.* **2007**, 3, 605-618.

(43) Wanko, M.; Hoffmann, M.; Frähmcke, J.; Frauenheim, T.; Elstner, M., Effect of Polarization on the Opsin Shift in Rhodopsins. 2. Empirical Polarization Models for Proteins. *J. Phys. Chem. B* **2008**, 112, 11468-11478.

(44) Altun, A.; Yokoyama, S.; Morokuma, K., Mechanism of Spectral Tuning Going from Retinal in Vacuo to Bovine Rhodopsin and its Mutants: Multireference ab Initio Quantum Mechanics/Molecular Mechanics Studies. *J. Phys. Chem. B* **2008**, 112, 16883-16890.

(45) Altun, A.; Yokoyama, S.; Morokuma, K., Spectral Tuning in Visual Pigments: An ONIOM(QM:MM) Study on Bovine Rhodopsin and its Mutants. *J. Phys. Chem. B* **2008**, 112, 6814-6827.

(46) Tomasello, G.; Olaso-González, G.; Altoè, P.; Stenta, M.; Serrano-Andrés, L.; Merchán, M.; Orlandi, G.; Bottoni, A.; Garavelli, M., Electrostatic Control of the Photoisomerization Efficiency and Optical Properties in Visual Pigments: On the Role of Counterion Quenching. *J. Am. Chem. Soc.* **2009**, 131, 5172-5186.

(47) Stenkamp, R. E.; Filipek, S.; Driessen, C. A. G. G.; Teller, D. C.; Palczewski, K., Crystal Structure of Rhodopsin: a Template for Cone Visual Pigments and Other G Protein-Coupled Receptors. *Biochim. Biophys. Acta* **2002**, 1565, 168-182.

(48) Asenjo, A. B.; Rim, J.; Oprian, D. D., Molecular Determinants of Human Red/Green Color Discrimination. *Neuron* **1994**, 12, 1131-1138.

(49) Svensson, M.; Humbel, S.; Froese, R. D. J.; Matsubara, T.; Sieber, S.; Morokuma, K., ONIOM: A Multilayered Integrated MO+MM Method for Geometry Optimizations and Single Point Energy Predictions. A Test for Diels-Alder Reactions and $Pt(P(t\text{-}Bu)_3)_2+H_2$ Oxidative Addition. *J. Phys. Chem.* **1996**, 100, 19357-19363.

(50) Wang, Z.; Asenjo, A. B.; Oprian, D. D., Identification of the Cl^--Binding Site in the Human Red and Green Color Vision Pigments. *Biochemistry* **1993**, 32, 2125-2130.

(51) Jumper, J.; Evans, R.; Pritzel, A.; Green, T.; Figurnov, M.; Ronneberger, O.; Tunyasuvunakool, K.; Bates, R.; Žídek, A.; Potapenko, A., et al., Highly accurate protein structure prediction with AlphaFold. *Nature* **2021**, 596, 583-589.

(52) Nakatsuji, H., Cluster expansion of the wavefunction. Excited states. *Chem. Phys. Lett.* **1978**, 59, 362-364.

(53) Yanai, T.; Tew, D. P.; Handy, N. C., A new hybrid exchange–correlation functional using the Coulomb-attenuating method (CAM-B3LYP). *Chem. Phys. Lett.* **2004**, 393, 51-57.

(54) Andersson, K.; Malmqvist, P. A.; Roos, B. O.; Sadlej, A. J.; Wolinski, K., Second-order perturbation theory with a casscf reference function. *J. Phys. Chem.* **1990**, 94, 5483-5488.

(55) Fujimoto, K. J.; Minoda, T.; Yanai, T., Spectral Tuning Mechanism of Photosynthetic Light-Harvesting Complex II Revealed by *Ab Initio* Dimer Exciton Model. *J. Phys. Chem. B* **2021**, 125, 10459-10470.

(56) Fujimoto, K. J., Electronic Couplings and Electrostatic Interactions Behind the Light Absorption of Retinal Proteins. *Front. Mol. Biosci.* **2021**, 8, 752700.